2011 American Control Conference
on O'Farrell Street, San Francisco, CA, USA
June 29 - July 01, 2011

Cumulative Retrospective Cost Adaptive Control of Systems with Amplitude and Rate Saturation

Benjamin J. Coffer[1], Jesse B. Hoagg[2], and Dennis S. Bernstein[3]

Abstract— **We demonstrate that the retrospective cost adaptive control algorithm can improve the tracking error when following square-wave and triangle-wave commands in the presence of amplitude and rate saturation, respectively, provided that the saturation level is known. Specifically, the retrospective cost adaptive control algorithm does not experience integrator windup, which is a common problem under amplitude and rate saturation for fixed-gain controllers with integral action.**

I. Introduction

Actuator saturation is unavoidable in control-system implementation due to physical constraints on stroke and power [1]. These constraints are responsible for amplitude saturation, which imposes limitations on the range of operation, and rate saturation, which imposes limitations on controller bandwidth. The extensive literature on saturation attests to the considerable effort devoted to this challenging and fundamental problem [2], [3].

In addition to the performance limitations of amplitude and rate saturation, linear control laws that are implemented without regard to saturation effects can result in unexpectedly adverse behavior. In particular, [4] shows that a stable closed-loop system may be rendered unstable by amplitude saturation. In addition, integral control for tracking or rejecting steps can experience integrator windup, which is a destabilizing effect [2], [3]. Consequently, an extensive literature has been devoted to antiwindup strategies, which typically disable the integrator during amplitude saturation [5]–[7].

An alternative approach to addressing the effects of saturation is to design a nonlinear controller that accounts for the presence of a saturation nonlinearity [6], [8]–[11]. In particular, a chain of three or more integrators cannot be stabilized by a saturated linear controller [12]; for such systems a nested saturation control [6] is needed. Not surprisingly, the sufficient conditions given in [13] for stability of a saturated linear control fail for plants with triple integrator dynamics.

The difficulties presented by saturation for fixed-gain controllers are exacerbated within the context of adaptive control, especially when the adaptation mechanism is not aware that saturation is present [14].

In the present paper, we consider both amplitude and rate saturation within the context of retrospective cost adaptive control (RCAC). RCAC uses a retrospective performance measure that facilitates controller adaptation with minimal assumptions about the plant and exogenous signals. In particular, RCAC is effective for adaptive control of nonminimum-phase systems provided that the nonminimum-phase zeros are known [15]–[17]. In this paper, we adopt the cumulative (i.e., recursive-least-squares) RCAC algorithm presented in [16]. A stability analysis of the algorithm is given in [17].

The goal of the present paper is to examine the stability and performance of RCAC in the presence of amplitude and rate saturation. To do this, we consider command following problems for square waves and triangle waves. We expect that RCAC will converge to an internal-model-type control law that incorporates either single-integrator or double-integrator dynamics. We stress that the adaptive controller will not be able to follow the commands with zero steady-state error because the amplitude and rate saturation makes this impossible. However, we intend to compare the steady-state performance of the adaptive controller to the steady-state performance of fixed-gain linear controllers. The goal of these investigations is to determine whether RCAC is susceptible to the destabilizing effects of integrator windup. The adaptive controller that we examine assumes that the saturation nonlinearity is known; the value of the saturated input is then used within the RCAC algorithm. Consequently, when the adaptive controller converges, the resulting fixed gain controller is a nonlinear compensator.

II. Command Following And Disturbance Rejection Problem

Consider the multi-input, multi-output system

$$x(k+1) = Ax(k) + Bu(k) + D_1 w(k), \tag{1}$$

$$y(k) = Cx(k) + D_2 w(k), \tag{2}$$

$$z(k) = E_1 x(k) + E_0 w(k), \tag{3}$$

where $x(k) \in \mathbb{R}^n$, $y(k) \in \mathbb{R}^{l_y}$, $z(k) \in \mathbb{R}^{l_z}$, $u(k) \in \mathbb{R}^{l_u}$, $w(k) \in \mathbb{R}^{l_w}$, and $k \geq 0$. Our goal is to develop an output feedback controller that generates a control signal u that minimizes the performance z in the presence of the exogenous signal w. We assume that measurements of the output y and the performance z are available for feedback; however, we assume that a direct measurement of the exogenous signal w is not available. Note that w can represent either a command signal to be followed, an external disturbance to be rejected, or both. In this paper, w represents a command signal. Let u_{c} be the commanded control signal, that is, the output of the feedback controller. In this paper, we consider the case where there is no saturation (i.e., $u = u_{\mathrm{c}}$) and the case where the commanded control u_{c} is either rate or amplitude saturated (i.e., $u \neq u_{\mathrm{c}}$).

[1]Graduate student, Department of Mechanical Engineering, The University of Michigan, Ann Arbor, MI 48109-2140, email: bcoffer@umich.edu

[2]Assistant Professor, Department of Mechanical Engineering, The University of Kentucky, Lexington, KY, 40506-0503, email: jhoagg@engr.uky.edu.

[3]Professor, Department of Aerospace Engineering, The University of Michigan, Ann Arbor, MI 48109-2140, email: dsbaero@umich.edu.

III. Command Following for Square and Triangle Waves Using Fixed-Gain Control

In this section, we present numerical examples to demonstrate single-integator and double-integrator windup using fixed-gain control. We demonstrate single-integrator windup using a controller with single-integral action to follow a square wave and double-integrator windup using a controller with double-integral action to follow a triangle wave. The numerical examples are constructed as follows:

(i) The exogenous commands $w(k)$ are either square waves or triangle waves. For $k \geq 0$, and $N = 0, 1, 2, \ldots$, we define the square wave

$$w_{\rm s}(k) \triangleq \begin{cases} +\frac{A_{\rm s}}{2}, & T_{\rm s}N \leq k < T_{\rm s}N + \frac{1}{2}T_{\rm s} \\ -\frac{A_{\rm s}}{2}, & T_{\rm s}N + \frac{1}{2}T_{\rm s} \leq k < T_{\rm s}N + T_{\rm s}, \end{cases}$$

and the triangle wave

$$w_{\rm t}(k) \triangleq \begin{cases} +A_{\rm s}\left[\frac{2}{T_{\rm s}}(k - T_{\rm s}N)\right], \\ \qquad \text{if } T_{\rm s}N - \frac{1}{4}T_{\rm s} \leq k < T_{\rm s}N + \frac{1}{4}T_{\rm s}, \\ -A_{\rm s}\left[\frac{2}{T_{\rm s}}(k - T_{\rm s}N) - 1\right], \\ \qquad \text{if } T_{\rm s}N + \frac{1}{4}T_{\rm s} \leq k < T_{\rm s}N + \frac{3}{4}T_{\rm s}, \end{cases}$$

where $T_{\rm s} = 2000$ time steps and $A_{\rm s} = 2$.

(ii) We assume that $z = y$.

(iii) (A, B, E_1) is a controllable canonical realization of the transfer function from u to z, $D_1 = 0_{n\times 1}$, and $E_0 = -1$. Therefore, (1)-(3) becomes $x(k+1) = Ax(k) + Bu(k)$ and $z(k) = E_1 x(k) - w(k)$, where objective is to have $y_{\rm out} \triangleq E_1 x$ follow w.

A. Square-wave command following for a minimum-phase plant with amplitude saturation

Consider the asymptotically stable, minimum-phase transfer function from u to z, given by

$$G_{zu}(\mathbf{z}) = \frac{(\mathbf{z} + 0.2 + 0.5\jmath)(\mathbf{z} + 0.2 - 0.5\jmath)}{(\mathbf{z} + 0.5 + 0.5\jmath)(\mathbf{z} + 0.5 - 0.5\jmath)(\mathbf{z} - 0.9)}. \quad (4)$$

The control objective is to have $y_{\rm out}$ follow the square-wave command $w = w_{\rm s}$. We consider the fixed-gain feedback $u_{\rm c} = G_{\rm PI}(\mathbf{z})z$, where

$$G_{\rm PI}(\mathbf{z}) \triangleq 0.2 + \frac{0.02}{\mathbf{z} - 1} = 0.2\frac{\mathbf{z} - 0.9}{\mathbf{z} - 1}. \quad (5)$$

The controller (5) is implemented in feedback with the plant (4), where $u_{\rm c}$ may experience amplitude saturatation, that is,

$$u(k) = \text{sgn}(u_{\rm c}(k)) \min(|u_{\rm c}(k)|, u_{\rm m}), \quad (6)$$

where $u_{\rm m} > 0$ is the amplitude saturation level. We consider the unsaturated case (i.e., $u_{\rm m} = \infty$) as well as four levels of amplitude saturation. Let $u_{\rm ss}$ be the steady-state command value required to achieve zero steady-state error. For the plant (4), $u_{\rm ss} \approx 0.15$. Next, we define four saturation levels, specifically, $u_{\rm m,10\%} = 0.9u_{\rm ss}$, $u_{\rm m,20\%} = 0.8u_{\rm ss}$, $u_{\rm m,40\%} = 0.6u_{\rm ss}$, and $u_{\rm m,80\%} = 0.2u_{\rm ss}$. Note that $u_{\rm m,10\%}$, $u_{\rm m,20\%}$, $u_{\rm m,40\%}$, and $u_{\rm m,80\%}$ are selected such that the unsaturated control signal $u_{\rm c}$ experiences approximately 10%, 20%, 40%, and 80% saturation, respectively, in comparison to $u_{\rm ss}$.

Figure 1 shows the time history of w, $y_{\rm out}$, $u_{\rm c}$, and u for the case without amplitude saturation as well as the cases where $u_{\rm m}$ equals $u_{\rm m,10\%}$, $u_{\rm m,20\%}$, $u_{\rm m,40\%}$, and $u_{\rm m,80\%}$. For the case without amplitude saturation, each time w changes sign, $y_{\rm out}$ experiences a transient and then approaches w, resulting in zero steady-state error. For the cases with amplitude saturation, Figure 1 shows that the amplitude saturation prevents $y_{\rm out}$ from following w with zero steady-state error. Furthermore, the unsaturated control signal $u_{\rm c}$ exhibits integrator windup. In particular, the integrator windup results in a phase lag in $y_{\rm out}$ changing direction to match the direction of the command w. Note that the effect of integrator windup increases as the amplitude saturation increases from 10% to 80%.

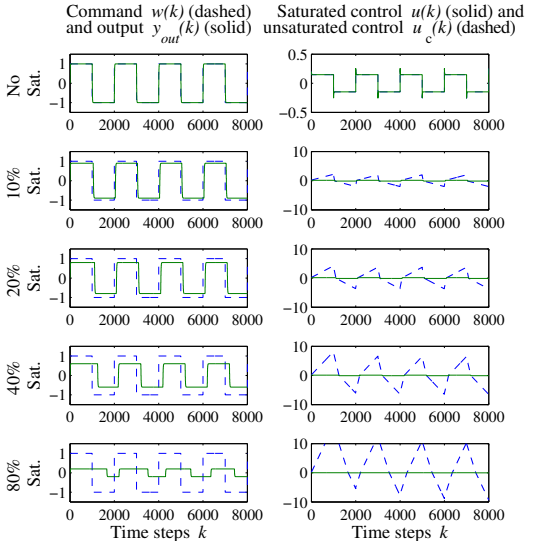

Fig. 1. *Square-wave command following for a minimum-phase plant with a proportional-integral controller.* The proportional-integral controller (5) is connected in feedback with (4). Five cases are considered from top to bottom, where the control signal has 0%, 10%, 20%, 40%, and 80% amplitude saturation. For the case without amplitude saturation, $y_{\rm out}$ follows w with zero steady-state error. For the cases with amplitude saturation, $y_{\rm out}$ is unable to follow w, and the unsaturated control signal $u_{\rm c}$ exhibits windup, which causes a phase lag in $y_{\rm out}$ relative to w.

B. Square-wave command following for a nonminimum-phase plant with amplitude saturation

Consider the asymptotically stable, nonminimum-phase transfer function from u to z, given by

$$G_{zu}(\mathbf{z}) = \frac{(\mathbf{z} + 1.1)(\mathbf{z} - 0.2)}{(\mathbf{z} - 0.5 + 0.5\jmath)(\mathbf{z} - 0.5 - 0.5\jmath)(\mathbf{z} + 0.7)}. \quad (7)$$

The control objective is to have $y_{\rm out}$ follow $w = w_{\rm s}$. We consider the fixed-gain feedback $u_{\rm c} = G_{\rm PI}(\mathbf{z})z$, where

$$G_{\rm PI}(\mathbf{z}) \triangleq 0.2 + \frac{0.08}{\mathbf{z} - 1} = 0.2\frac{\mathbf{z} - 0.6}{\mathbf{z} - 1}. \quad (8)$$

The controller (8) is implemented in feedback with (7), where the control signal $u_{\rm c}$ may be amplitude saturated, as given by (6), where $u_{\rm ss} \approx 0.5$ for the plant (7).

Figure 2 shows the time history of w, $y_{\rm out}$, $u_{\rm c}$, and u for the cases with and without amplitude saturation. The results are similar to those shown in Figure 1.

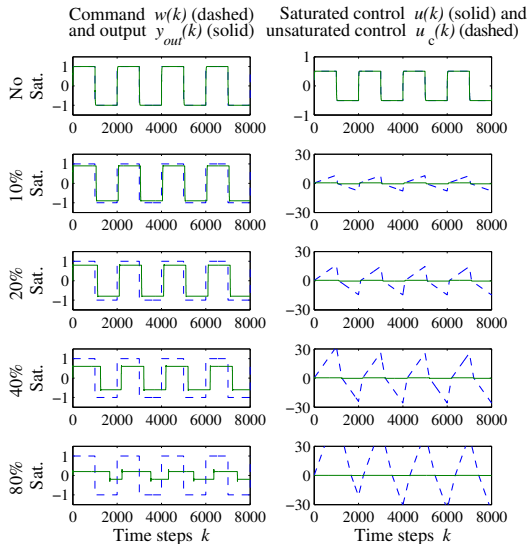

Fig. 2. *Square-wave command following for a nonminimum-phase plant with a proportional-integral controller.* The proportional-integral controller (8) is connected in feedback with (7). Five cases are considered from top to bottom, where the control signal has 0%, 10%, 20%, 40%, and 80% amplitude saturation. For the case without amplitude saturation, $y_{\rm out}$ follows w with zero steady-state error. For the cases with amplitude saturation, $y_{\rm out}$ is unable to follow w, and the unsaturated control signal $u_{\rm c}$ exhibits windup, which causes a phase lag in $y_{\rm out}$ relative to w.

C. Triangle-wave command following for a minimum-phase plant with rate saturation

In this section, we reconsider (4), where the objective is to have $y_{\rm out}$ follow the triangle-wave command $w = w_{\rm t}$. We consider the feedback $u_{\rm c} = G_{\rm PII}(\mathbf{z})z$, where

$$G_{\rm PII}(\mathbf{z}) \triangleq 0.2 + \frac{0.2(\mathbf{z}-0.91)}{(\mathbf{z}-1)^2}. \tag{9}$$

The controller (9) is implemented in feedback with (4), where the control signal $u_{\rm c}$ may be rate saturated, that is,

$$u(k) = \begin{cases} u_{\rm c}(k), & |\delta(k)| \le \Delta u_{\rm m} \\ u(k-1) + \operatorname{sgn}(\delta(k))\Delta u_{\rm m}, & |\delta(k)| > \Delta u_{\rm m}, \end{cases} \tag{10}$$

where $\delta(k) \triangleq u_{\rm c}(k) - u(k-1)$ and $\Delta u_{\rm m} > 0$ is the rate saturation level, that is, the maximum allowable control-signal move size. We consider the unsaturated case (i.e., $\Delta u_{\rm m} = \infty$) as well as four levels of rate saturation. Let $\Delta u_{\rm ss}$ be the steady-state rate required by the command to achieve zero steady-state tracking error. For the plant (4), $\Delta u_{\rm ss} \approx 0.0003$. Next, we define four saturation levels, specifically, $\Delta u_{\rm m,10\%} = 0.9\Delta u_{\rm ss}$, $\Delta u_{\rm m,20\%} = 0.8\Delta u_{\rm ss}$, $\Delta u_{\rm m,40\%} = 0.6\Delta u_{\rm ss}$, and $\Delta u_{\rm m,80\%} = 0.2\Delta u_{\rm ss}$. Note that $\Delta u_{\rm m,10\%}$, $\Delta u_{\rm m,20\%}$, $\Delta u_{\rm m,40\%}$, and $\Delta u_{\rm m,80\%}$ are selected such that the unsaturated control signal $u_{\rm c}$ experiences approximately 10%, 20%, 40%, and 80% rate saturation, respectively, in comparison to $\Delta u_{\rm ss}$.

Figure 3 shows the time history of w, $y_{\rm out}$, $u_{\rm c}$, and u for the case without rate saturation as well as the cases where $\Delta u_{\rm m}$ equals $\Delta u_{\rm m,10\%}$, $\Delta u_{\rm m,20\%}$, $\Delta u_{\rm m,40\%}$, and $\Delta u_{\rm m,80\%}$. For the case without rate saturation, $y_{\rm out}$ follows w with zero steady-state error. For the cases with rate saturation, Figure 3 shows that the closed-loop system is internally unstable due to double-integrator windup. More specifically, $u_{\rm c}$ diverges.

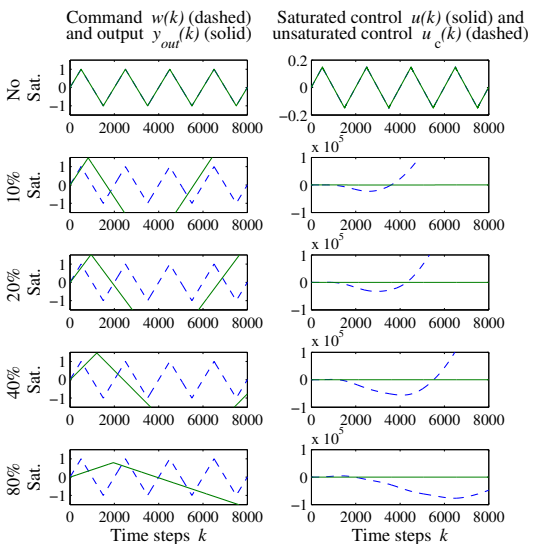

Fig. 3. *Triangle-wave command following for a minimum-phase plant with a proportional-double-integral controller.* The proportional-double-integral controller (9) is connected in feedback with (4). Five cases are considered from top to bottom, where the control signal has 0%, 10%, 20%, 40%, and 80% rate saturation. For the case without rate saturation, $y_{\rm out}$ follows w with zero steady-state error. For the cases with rate saturation, the closed-loop system is internally unstable due to double-integrator windup, that is, $u_{\rm c}$ diverges.

D. Triangle-wave command following for a nonminimum-phase plant with rate saturation

In this section, we reconsider (7), where the control objective is to have $y_{\rm out}$ follow $w = w_{\rm t}$. We consider the feedback $u_{\rm c} = G_{\rm PII}(\mathbf{z})z$, where

$$G_{\rm PII}(\mathbf{z}) \triangleq 0.4 + \frac{0.36(\mathbf{z}-2/3)}{(\mathbf{z}-1)^2}. \tag{11}$$

The controller (11) is implemented in feedback with (7), where the control signal $u_{\rm c}$ may be rate saturated, as given by (10), where $\Delta u_{\rm ss} \approx 0.001$ for the plant (7).

Figure 4 shows the time history of w, $y_{\rm out}$, $u_{\rm c}$, and u for the cases with and without rate saturation. The results are similar to those shown in Figure 3.

IV. Retrospective Cost Adaptive Control

In this section, we review the cumulative retrospective cost adaptive control (RCAC) algorithm presented in [16], [17]. First, we represent (1) and (3) as the time-series model

$$z(k) = \sum_{i=1}^{n} -\alpha_i z(k-i) + \sum_{i=d}^{n} \beta_i u(k-i) + \sum_{i=0}^{n} \gamma_i w(k-i),$$

where $\alpha_1, \ldots, \alpha_n \in \mathbb{R}$, $\beta_d, \ldots, \beta_n \in \mathbb{R}^{l_z \times l_u}$, $\gamma_0, \ldots, \gamma_n \in \mathbb{R}^{l_z \times l_w}$, and the relative degree is $d > 0$.

Next, consider the time-series controller given by

$$u_{\rm c}(k) = \sum_{i=1}^{n_{\rm c}} M_i(k) u_{\rm c}(k-i) + \sum_{i=1}^{n_{\rm c}} N_i(k) y(k-i), \tag{12}$$

where, for all $i = 1, \ldots, n_{\rm c}$, $M_i : \mathbb{N} \to \mathbb{R}^{l_u \times l_u}$ and $N_i : \mathbb{N} \to \mathbb{R}^{l_u \times l_y}$ are determined by the adaptive control

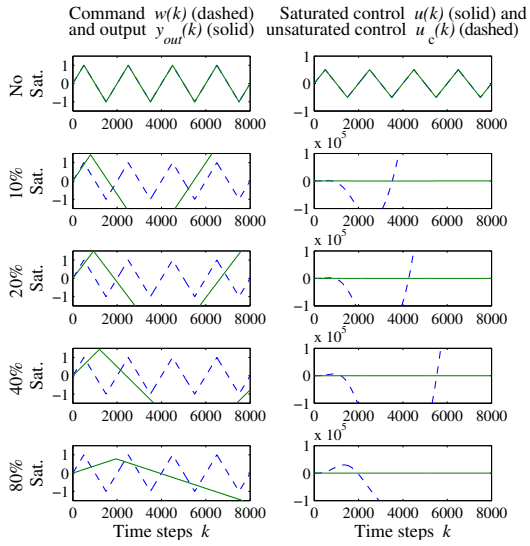

Fig. 4. *Triangle-wave command following for a nonminimum-phase plant with a proportional-double-integral controller.* The proportional-double-integral controller (11) is connected in feedback with (7). Five cases are considered from top to bottom, where the control signal has 0%, 10%, 20%, 40%, and 80% rate saturation. For the case without rate saturation, $y_{\rm out}$ follows w with zero steady-state error. For the cases with rate saturation, the closed-loop system is internally unstable due to double-integrator windup, that is, $u_{\rm c}$ diverges.

law presented below. The control (12) can be expressed as $u_{\rm c}(k) = \theta_{\rm c}(k)\phi(k)$, where

$$\theta_{\rm c}(k) \triangleq \left[\begin{array}{cccccccc} N_1(k) & \cdots & N_{n_{\rm c}}(k) & M_1(k) & \cdots & M_{n_{\rm c}}(k) \end{array} \right],$$
$$\phi(k) \triangleq \left[\begin{array}{cccc} y^{\rm T}(k-1) & \cdots & y^{\rm T}(k-n_{\rm c}) \\ u_{\rm c}^{\rm T}(k-1) & \cdots & u_{\rm c}^{\rm T}(k-n_{\rm c}) \end{array} \right]^{\rm T}. \tag{13}$$

Next, we define the retrospective performance

$$\hat{z}(\hat{\theta}_{\rm c}, k) \triangleq z(k) + \sum_{i=d}^{\nu} \bar{\beta}_i \left[\hat{\theta}_{\rm c} - \theta_{\rm c}(k-i) \right] \phi(k-i),$$

where $\nu \geq d$, $\hat{\theta}_{\rm c} \in \mathbb{R}^{l_u \times (n_{\rm c}(l_y+l_u))}$ is an optimization variable used to derive the adaptive law, and $\bar{\beta}_d, \ldots, \bar{\beta}_\nu \in \mathbb{R}^{l_z \times l_u}$. The parameters ν and $\bar{\beta}_d, \ldots, \bar{\beta}_\nu$ must capture the information included in the first nonzero Markov parameter and the nonminimum-phase zeros from u to z [16]. In this paper, we let $\bar{\beta}_d, \ldots, \bar{\beta}_\nu$ be the coefficients of the portion of the numerator polynomial matrix $\beta(\mathbf{z}) \triangleq \mathbf{z}^{n-d}\beta_d + \mathbf{z}^{n-d-1}\beta_{d+1} + \cdots + \mathbf{z}\beta_{n-1} + \beta_n$ that includes the nonminimum-phase transmission zeros. Specifically, let $\beta(\mathbf{z})$ have the polynomial matrix factorization $\beta(\mathbf{z}) = \beta_{\rm u}(\mathbf{z})\beta_{\rm s}(\mathbf{z})$, where $\beta_{\rm u}(\mathbf{z})$ is an $l_z \times l_u$ polynomial matrix of degree $n_{\rm u} \geq 0$ whose leading matrix coefficient is β_d, $\beta_{\rm s}(\mathbf{z})$ is a monic $l_u \times l_u$ polynomial matrix of degree $n - n_{\rm u} - d$, and each Smith zero of $\beta(\mathbf{z})$ counting multiplicity that lies on or outside the unit circle is a Smith zero of $\beta_{\rm u}(\mathbf{z})$. Next, we can write $\beta_{\rm u}(\mathbf{z}) = \beta_{{\rm u},0}\mathbf{z}^{n_{\rm u}} + \beta_{{\rm u},1}z^{n_{\rm u}-1} + \cdots + \beta_{{\rm u},n_{\rm u}-1}z + \beta_{{\rm u},n_{\rm u}}$, where $\beta_{{\rm u},0} \triangleq \beta_d$. In this case, we let $\nu = n_{\rm u} + d$ and for $i = d, \ldots, n_{\rm u} + d$, $\bar{\beta}_i = \beta_{{\rm u},i-d}$.

Defining $\hat{\Theta}_{\rm c} \triangleq \mathrm{vec}\, \hat{\theta}_{\rm c} \in \mathbb{R}^{n_{\rm c}l_u(l_y+l_u)}$ and $\Theta_{\rm c}(k) \triangleq \mathrm{vec}\, \theta_{\rm c}(k) \in \mathbb{R}^{n_{\rm c}l_u(l_y+l_u)}$, it follows that

$$\hat{z}(\hat{\Theta}_{\rm c}, k) = z(k) - \sum_{i=d}^{\nu} \Phi_i^{\rm T}(k)\Theta_{\rm c}(k-i) + \Psi^{\rm T}(k)\hat{\Theta}_{\rm c},$$

where, for $i = d, \ldots, \nu$, $\Phi_i(k) \triangleq \phi(k-i) \otimes \bar{\beta}_i^{\rm T} \in \mathbb{R}^{(n_{\rm c}l_u(l_y+l_u)) \times l_z}$, where $\otimes$ represents the Kronecker product, and $\Psi(k) \triangleq \sum_{i=d}^{\nu} \Phi_i(k)$.

Now, define the cumulative retrospective cost function

$$J(\hat{\Theta}_{\rm c}, k) \triangleq \sum_{i=0}^{k} \lambda^{k-i} \hat{z}^{\rm T}(\hat{\Theta}_{\rm c}, i) R \hat{z}(\hat{\Theta}_{\rm c}, i) + \lambda^k (\hat{\Theta}_{\rm c} - \Theta_{\rm c}(0))^{\rm T} Q (\hat{\Theta}_{\rm c} - \Theta_{\rm c}(0)), \tag{14}$$

where $\lambda \in (0, 1]$, and $R \in \mathbb{R}^{l_z \times l_z}$ and $Q \in \mathbb{R}^{(n_{\rm c}l_u(l_y+l_u)) \times (n_{\rm c}l_u(l_y+l_u))}$ are positive definite.

The cumulative retrospective cost function (14) is minimized by a recursive least-squares (RLS) algorithm with a forgetting factor. Therefore, for each $k \geq 0$, $J(\hat{\Theta}_{\rm c}, k)$ is minimized by the adaptive law

$$\Theta_{\rm c}(k+1) = \Theta_{\rm c}(k) - P(k)\Psi(k)\Omega(k)^{-1} z_{\rm R}(k), \tag{15}$$
$$P(k+1) = \frac{1}{\lambda}\left[P(k) - P(k)\Psi(k)\Omega(k)^{-1}\Psi^{\rm T}(k)P(k) \right], \tag{16}$$

where $\Omega(k) \triangleq \lambda R^{-1} + \Psi^{\rm T}(k)P(k)\Psi(k)$, $P(0) = Q^{-1}$, $\Theta_{\rm c}(0) \in \mathbb{R}^{n_{\rm c}l_u(l_y+l_u)}$, and $z_{\rm R}(k) \triangleq \hat{z}(\Theta_{\rm c}(k), k)$. The cumulative RCAC algorithm is thus given by (15), (16), and

$$u_{\rm c}(k) = \theta_{\rm c}(k)\phi(k) = \mathrm{vec}^{-1}(\Theta_{\rm c}(k))\phi(k). \tag{17}$$

V. RCAC With Rate And Amplitude Saturation

We adjust RCAC (15)-(17) to account for rate and amplitude saturation. More specifically, we assume that the adaptive algorithm has a measurement of the saturated control u. In this case, the saturated control u is used to construct ϕ in place of the unsaturated control $u_{\rm c}$. More specifically, we replace ϕ given by (13) with

$$\phi(k) \triangleq \left[\begin{array}{cccc} y^{\rm T}(k-1) & \cdots & y^{\rm T}(k-n_{\rm c}) \\ u^{\rm T}(k-1) & \cdots & u^{\rm T}(k-n_{\rm c}) \end{array} \right]^{\rm T}.$$

No additional alterations to the controller construction are required. Note that it follows from (17) that the resulting control law is nonlinear even in the case where the adaptive gains $\theta(k)$ have converged and are constant.

VI. Command Following Using RCAC

In this section, we revisit the square-wave and triangle-wave command following problems presented in Section III, using RCAC rather than a fixed-gain controller. We demonstrate that RCAC can mitigate the effect of windup. The adaptive controller is not able to follow the commands with zero steady-state error because the amplitude and rate saturation makes this impossible. However, numerical simulations demonstrate that the internal states of the adaptive controller remain bounded unlike the fixed-gain controllers

of Section III, where integrator windup caused $u_{\rm c}$ to diverge in some instances. The numerical examples in this section are constructed under assumptions *(i)-(iii)* from Section III. In addition, $\theta(0) = 0$ and $\lambda = 1$.

A. Square-wave command following for a minimum-phase plant with amplitude saturation

Reconsider the square-wave command following problem given in Section III-A for (4). The adaptive controller (15)-(17) is implemented in feedback with $n_{\rm c} = 10$ and $P(0) = I_{20}$. Since (4) is minimum phase, we let $\nu = d = 1$ and $\bar{\beta}_1 = \beta_1 = 1$. Figure 5 shows the time history of w, $y_{\rm out}$, $u_{\rm c}$, and u for the case without amplitude saturation as well as the cases where $u_{\rm m}$ equals $u_{{\rm m},10\%}$, $u_{{\rm m},20\%}$, $u_{{\rm m},40\%}$, and $u_{{\rm m},80\%}$. For the case without amplitude saturation, there is zero steady-state error, and the performance is comparable to that of the fixed-gain controller (5) shown in Figure 1. For the cases with amplitude saturation, Figure 5 shows that the amplitude saturation prevents $y_{\rm out}$ from following w with zero steady-state error. However, $u_{\rm c}$ does not exhibit integrator windup, and $y_{\rm out}$ is able to shift direction to match the direction of w without phase lag. This compares favorably with the fixed-gain proportional-integral controller used in Figure 1.

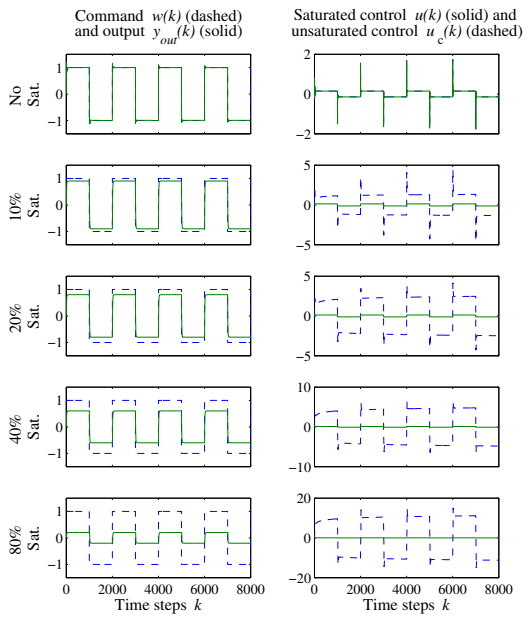

Fig. 5. *Square-wave command following for a minimum-phase plant with RCAC.* The adaptive control (15)-(17) with $n_{\rm c} = 10$ and $P(0) = I_{20}$ is connected in feedback with (4). Five cases are considered from top to bottom, where the control signal has 0%, 10%, 20%, 40%, and 80% amplitude saturation. For the case without amplitude saturation, $y_{\rm out}$ follows the command w with zero steady-state error. For the cases with amplitude saturation, $y_{\rm out}$ is unable to follow w. However, $u_{\rm c}$ does not exhibit integrator windup, and $y_{\rm out}$ is able to shift direction to match the direction of w without phase lag.

B. Square-wave command following for a nonminimum-phase plant with amplitude saturation

Reconsider the square-wave command following problem given in Section III-B for (7). RCAC is implemented in feedback with $n_{\rm c} = 10$ and $P(0) = I_{20}$. Since (7) is nonminimum phase, we let $\nu = d+n_{\rm u} = 2$ and $\bar{\beta}_1 = \beta_1 = 1$, and $\bar{\beta}_2 = \beta_{{\rm u},1} = -1.1$. Figure 6 shows the time history of w, $y_{\rm out}$, $u_{\rm c}$, and u for the cases with and without amplitude saturation. For the case without amplitude saturation, there is zero steady-state error, and the performance is comparable to that of the fixed-gain controller (8) shown in Figure 2. For the cases with amplitude saturation, $y_{\rm out}$ is unable to follow w with zero steady-state error. However, $u_{\rm c}$ does not exhibit integrator windup, and $y_{\rm out}$ is able to shift direction to match the direction of w without phase lag. This compares favorably with the fixed-gain controller used in Figure 2.

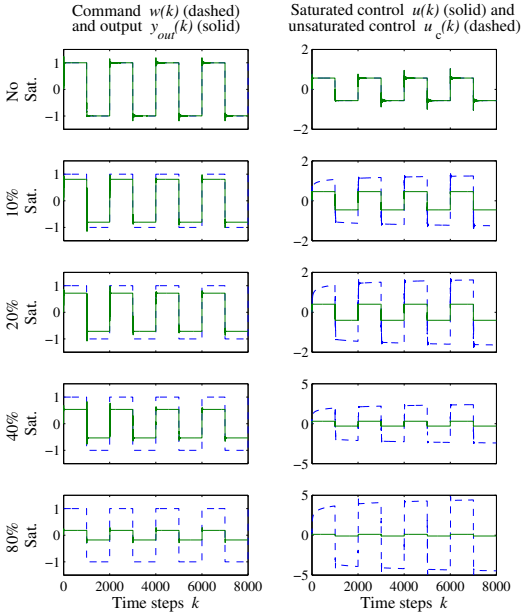

Fig. 6. *Square-wave command following for a minimum-phase plant with RCAC.* The adaptive control (15)-(17) with $n_{\rm c} = 10$, and $P(0) = I_{20}$ is connected in feedback with (7). Five cases are considered from top to bottom, where the control signal has 0%, 10%, 20%, 40%, and 80% amplitude saturation. For the case without amplitude saturation, $y_{\rm out}$ follows the command w with zero steady-state error. For the cases with amplitude saturation, $y_{\rm out}$ is unable to follow w. However, $u_{\rm c}$ does not exhibit integrator windup, and $y_{\rm out}$ is able to shift direction to match the direction of w without phase lag.

C. Triangle-wave command following for a minimum-phase plant with rate saturation

Reconsider the triangle-wave command following problem given in Section III-C for (4). RCAC is implemented in feedback with $n_{\rm c} = 10$ and $P(0) = I_{20}$. Since (4) is minimum phase, we let $\nu = d = 1$ and $\bar{\beta}_1 = \beta_1 = 1$. Figure 7 shows the time history of w, $y_{\rm out}$, $u_{\rm c}$, and u for the case without rate saturation as well as the cases where $\Delta u_{\rm m}$ equals $\Delta u_{{\rm m},10\%}$, $\Delta u_{{\rm m},20\%}$, $\Delta u_{{\rm m},40\%}$, and $\Delta u_{{\rm m},80\%}$. For the case without rate saturation, there is zero steady-state error, and the performance is comparable to that of the fixed-gain controller (9) shown in Figure 3. For the cases with rate saturation, Figure 7 shows that the rate saturation prevents $y_{\rm out}$ from following w with zero steady-state error. However, $u_{\rm c}$ does not exhibit integrator windup. In particular, the closed-loop system maintains stability and $u_{\rm c}$ does not diverge as it did with the fixed-gain proportional-double-integral controller as shown in Figure 3.

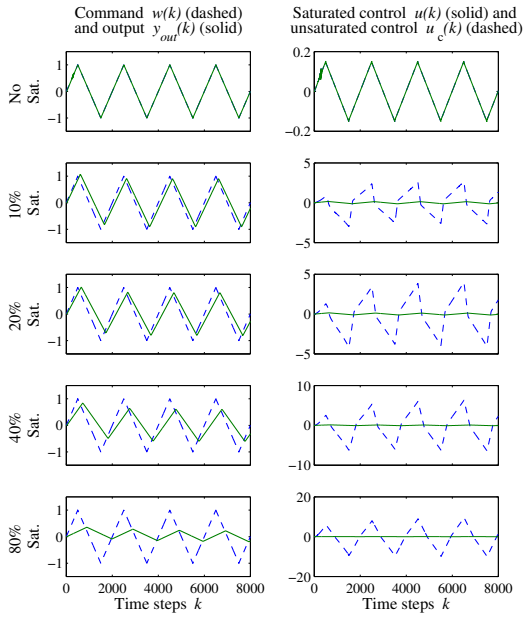

Fig. 7. *Triangle-wave command following for a minimum-phase plant with RCAC.* The adaptive control (15)-(17) with $n_c = 10$ and $P(0) = I_{20}$ is connected in feedback with (4). Five cases are considered from top to bottom, where the control signal has 0%, 10%, 20%, 40%, and 80% rate saturation. For the case without rate saturation, $y_{\rm out}$ follows w with zero steady-state error. For the cases with rate saturation, $y_{\rm out}$ is unable to follow w; however, the unsaturated control signal $u_{\rm c}$ remains bounded.

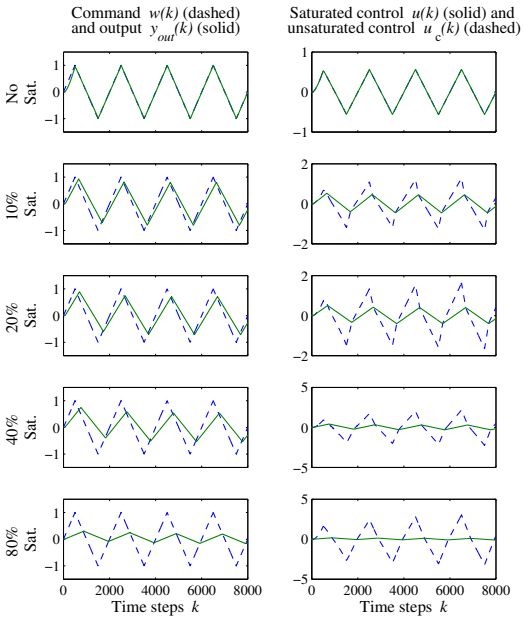

Fig. 8. *Triangle-wave command following for a minimum-phase plant with RCAC.* The adaptive control (15)-(17) with $n_c = 10$ and $P(0) = 0.01I_{20}$ is connected in feedback with (7). Five cases are considered from top to bottom, where the control signal has 0%, 10%, 20%, 40%, and 80% rate saturation. For the case without rate saturation, $y_{\rm out}$ follows w with zero steady-state error. For the cases with rate saturation, $y_{\rm out}$ is unable to follow w; however, the unsaturated control signal $u_{\rm c}$ remains bounded.

D. Triangle-wave command following for a nonminimum-phase plant with rate saturation

Reconsider the triangle-wave command following problem given in Section III-D for (7). RCAC is implemented in feedback with $n_{\rm c} = 10$ and $P(0) = 0.01I_{20}$. Since (7) is nonminimum phase, we let $\nu = d+n_{\rm u} = 2$ and $\bar{\beta}_1 = \beta_1 = 1$, and $\bar{\beta}_2 = \beta_{{\rm u},1} = -1.1$. Figure 8 shows the time history of w, $y_{\rm out}$, $u_{\rm c}$, u for the cases with and without rate saturation. For the case without rate saturation, there is zero steady-state error, and the performance is comparable to that of the fixed-gain controller (11) shown in Figure 4. For the cases with rate saturation, $y_{\rm out}$ is unable to follow w with zero steady-state error. However, $u_{\rm c}$ does not exhibit integrator windup. In particular, the closed-loop system maintains stability and $u_{\rm c}$ does not diverge as it did with the fixed-gain proportional-double-integral controller as shown in Figure 4.

VII. Conclusion

This paper demonstrated that RCAC is effective for handling amplitude and rate saturation, and does not displace integrator windup. Future work includes a stability analysis of RCAC under amplitude and rate saturation.

References

[1] Y. Wang and R. M. Murray, "Bifurcation control of rotating stall with actuator magnitude and rate limits: Part I-model reduction and qualitative dynamics," *Automatica*, vol. 38, pp. 597–610, 2002.

[2] V. Kapila and K. M. Grigoriadis, Eds., *Actuator Saturation Control*. CRC Press, 2002.

[3] A. H. Glattfelder and W. Schaufelberger, *Control Systems with Input and Output Constraints*. Springer, 2003.

[4] B. Aguirre, J. Alvarez-Ramirez, G. Fernandez, and R. Suarez, "First Harmonic Analysis of Linear Control Systems with High-Gain Saturating Feedback," *Int. J. Bifurcation Chaos*, vol. 7, pp. 2501–2510, 1997.

[5] M. V. Kothare, P. J. Campo, M. Morari, and C. N. Nett, "A unified framework for the study of anti-windup designs," *Automatica*, vol. 30, pp. 1869–1883, 1994.

[6] A. R. Teel, "Global stabilization and restricted tracking for multiple integrators with bounded controls," *Sys. Contr. Lett.*, vol. 18, pp. 165–171, 1992.

[7] Y.-Y. Cao, Z. Lin, and D. G. Ward, "An antiwindup approach to enlarging domain of attraction for linear systems subject to actuator saturation," *IEEE Trans. Autom. Contr.*, vol. 47, pp. 140–145, 2002.

[8] D. S. Bernstein and W. M. Haddad, "Nonlinear Controllers for Positive Real Systems with Arbitrary Input Nonlinearities," *IEEE Trans. Autom. Contr.*, vol. 39, pp. 1513–1517, 1994.

[9] F. Tyan and D. S. Bernstein, "Dynamic Output Feedback Compensation for Systems with Independent Amplitude and Rate Saturations," *Int. J. Contr.*, vol. 67, pp. 89–116, 1997.

[10] R. M. Murray, *The Astrom Symposium on Control*. Studentlitteratur Lund, 1999, ch. Geometric approaches to control in the presence of magnitude and rate saturations, ISBN: 91-44-01245-4.

[11] E. G. Gilbert, I. Kolmanovsky, and K. T. Tan, "Discrete-time reference governors and the nonlinear control of systems with state and control constraints," *Int. J. Robust Nonlinear Contr.*, vol. 5, pp. 487–504, 1994.

[12] A. T. Fuller, "In-the-large stability of relay and saturating control systems with linear controllers," *Int. J. Contr.*, vol. 10, pp. 457–480, 1969.

[13] F. Tyan and D. S. Bernstein, "Global Stabilization of Systems Containing a Double Integrator Using a Saturated Linear Controller," *Int. J. Robust Nonlinear Contr.*, vol. 9, pp. 1143–1156, 1999.

[14] A. M. Annaswamy and J.-E. Wong, "Adaptive control in the presence of saturation non-linearity," *Int. J. Adaptive Contr. Sig. Proc.*, vol. 11, pp. 3–19, 1998.

[15] M. A. Santillo and D. S. Bernstein, "Adaptive control based on retrospective cost optimization," *AIAA J. Guid. Contr. Dyn.*, vol. 33, pp. 289–304, 2010.

[16] J. B. Hoagg and D. S. Bernstein, "Cumulative retrospective cost adaptive control with RLS-based optimization," in *Proc. Amer. Contr. Conf.*, Baltimore, MD, June 2010, pp. 4016–4021.

[17] ——, "Retrospective cost adaptive control for nonminimum-phase discrete-time systems, Part 1 and Part 2," in *Proc. Conf. Dec. Contr.*, Atlanta, GA, December 2010, pp. 893–904.